Applied Physics Letters

Photoacoustic detection of low duty cycle gratings through optically opaque layers

Cite as: Appl. Phys. Lett. **117**, 051104 (2020); https://doi.org/10.1063/5.0016078
Submitted: 01 June 2020 . Accepted: 23 July 2020 . Published Online: 07 August 2020

V. Verrina, S. Edward, H. Zhang, S. Witte, and P. C. M. Planken

Applied Physics Letters ARTICLE scitation.org/journal/apl

Photoacoustic detection of low duty cycle gratings through optically opaque layers

Cite as: Appl. Phys. Lett. **117**, 051104 (2020); doi: 10.1063/5.0016078
Submitted: 1 June 2020 · Accepted: 23 July 2020 ·
Published Online: 7 August 2020

View Online Export Citation CrossMark

V. Verrina,[1,2,a)] S. Edward,[1,2] H. Zhang,[1,3] S. Witte,[1,3] and P. C. M. Planken[1,2,b)]

AFFILIATIONS

[1]Advanced Research Centre for Nanolithography (ARCNL), Science Park 106, 1098 XG Amsterdam, The Netherlands
[2]Van der Waals-Zeeman Institute, University of Amsterdam, Science Park 904, 1098 XH Amsterdam, The Netherlands
[3]Department of Physics and Astronomy, Vrije Universiteit, De Boelelaan 1081, 1081 HV Amsterdam, The Netherlands

[a)]**Author to whom correspondence should be addressed:** v.verrina@arcnl.nl
[b)]**Electronic mail:** p.planken@arcnl.nl

ABSTRACT

We report on the use of ultra-high frequency photoacoustics to detect gratings with linewidths as narrow as 75 nm, buried underneath optically opaque metal layers. Our results show that buried gratings can be detected by observing diffraction from the spatially periodic acoustic replica of the buried grating at the glass/metal interface and from replicas of the acoustic wave inside the glass substrate. The measured diffraction signals show a linear dependence on grating duty cycle rather than the expected quadratic one. We find that this is due to the presence of a coherent background optical field, which interferes with and coherently amplifies the weaker fields diffracted off the grating-shaped acoustic waves. Our measurements show that ultra-high frequency photoacoustics is a promising technique for detection of sub-wavelength periodic nanostructures.

In nanolithography, semiconductor devices are fabricated by exposing a photoresist on a Si wafer in a multi-layer fashion. This requires that the wafer is positioned ("aligned") with an accuracy of less than a nanometer to ensure, for example, functioning vertical interconnects between layers. Wafer alignment is typically done by measuring optical diffraction off gratings etched in scribe lanes between the dies on a Si wafer.[1,2] When the wafer position changes in a direction along the grating wavevector, the phase of the optical beams diffracted off these gratings changes. By measuring these changes, the (relative) position of the wafer can be determined accurately.[3] In the fabrication process, however, alignment becomes challenging when these gratings get covered with layers of materials that are not, or are only partially, transparent to light. Recently, we showed how laser-induced ultrasound with frequencies of tens to hundreds of GHz (see also Refs. 4–18) can be used to detect gratings buried below optically opaque layers.[19,20] In this technique, diffraction off an acoustic replica of the buried grating is used to detect the presence of the optically hidden grating. In this way, we were able to detect buried gratings even after propagation of the acoustic wave through as many as 2 × 20 dielectric layers. The gratings, however, all had fairly large linewidths of 3 μm. Little is known about the ability of the technique to detect buried gratings with much narrower linewidths. This topic has gained importance in view of the tendency in the semiconductor manufacturing industry to move toward smaller-period alignment gratings with narrow lines, which occupy less wafer space. In principle, ultra-high frequency acoustic waves can have wavelengths in the tens to hundreds of nanometer range, considerably shorter than the wavelengths of visible light, and should, thus, also be sensitive to the presence of very narrow grating lines.

Here, we show the results of photoacoustic measurements to detect gratings with duty cycle as low as 1.25%, buried underneath an opaque layer. We find that, even for grating lines as narrow as 75 nm, weak but measurable diffraction signals are observed. This is surprising because the measured diffraction efficiency is much higher for these linewidths than expected from just the acoustic replicas of the buried gratings, which are calculated to have diffraction efficiencies in the range of 10^{-12}–10^{-11}. Our results can be explained by the presence of a coherent background scattered optical field, which interferes with and amplifies the optical fields diffracted off the acoustic-wave-induced gratings. This leads to measurable diffraction signals, which periodically drop below the background signal level and give rise to a linear rather than the expected quadratic dependence of the diffracted

signal strength as a function of the grating duty cycle. Our measurements are in excellent agreement with numerical simulations that take the generation, propagation, diffraction, and optical detection of the acoustic waves into account. The results illustrate the potential of photoacoustics to detect nanostructures buried below optically opaque layers for the semiconductor device manufacturing industry.

Our experiments were performed using a pump-probe setup. The laser is a Ti:sapphire oscillator generating 70 fs pulses at a repetition rate of 5.1 MHz, centered at a wavelength of 800 nm. The laser output is split into two. One part is frequency doubled to generate 400 nm pump pulses. The other 800 nm beam is used as the probe. The time delay between the pump and the probe is varied by changing the optical path length with a mechanical delay stage on which two mirrors are mounted in a retro-reflecting geometry. The first-order diffracted probe beam is measured by a Si photodiode. It has a bandwidth of about 50 kHz and thus continuously integrates over about 100 laser pulses. Changes in the strength of the resulting electronic signal are only caused by pump-induced changes in the signal when the pump-probe delay is slowly varied. To further suppress noise, a chopper modulates the pump beam with a frequency of 6 kHz and the lock-in amplifier, set at an integration time of 3 ms, detects only that part of the probe signal that is modulated at 6 kHz. The delay stage moves in a continuous, relatively slow fashion, and care was taken to limit scanning the delay too quickly to avoid smearing out of fast features in the measurements due to the 3 ms integration time of the lock-in amplifier. The pump beam has a spot size of 50 μm diameter on the sample and has an average power that varies from 20 to 50 mW, depending on the experiment. The probe has a spot size of 40 μm diameter, and its power was kept constant at about 60 mW. Note that, anticipating weak signals, every attempt was made to enhance the signal, including using a very strong probe pulse. Our gratings are fabricated using e-beam lithography, on top of a Au layer deposited on a glass substrate. By performing the pump-probe measurements from the glass side [Fig. 1], the gratings are optically invisible to the laser pulses and can be considered "buried." Most importantly, since at this interface the Au is essentially flat, we avoid any residual topography grating, which could lead to a relatively strong constant optical diffraction. Note that in real semiconductor device manufacturing, Si is often used as a substrate and although Si absorbs 400 and 800 nm light, longer wavelengths could, in principle, also be used in a range where the Si is transparent. However, excitation from the front surface is also possible and, in fact, a better choice because it is more compatible with existing metrology solutions. Two sets of five different Au gratings were fabricated, one set on a 90 nm thick flat Au layer and the other on a 142 nm thick flat Au layer. All five gratings in a set have an amplitude of 44 nm, a period of 6 μm, but different duty cycle of 1.25%, 2.08%, 4.16%, 8.33%, and 16.66%, corresponding to ridge linewidths of 75 nm, 125 nm, 250 nm, 500 nm, and 1 μm, respectively. Scanning Electron Microscope (SEM) images of two gratings with linewidths of 1 μm and 75 nm are shown in the inset of Fig. 1.

In Fig. 2, we plot the first-order diffracted probe signal as a function of the delay between pump and probe pulses for the five Au gratings fabricated on a 90 nm thick Au layer (solid colored lines in top five panels). While performing these measurements, a significant variation of the diffracted signal strength was observed as a function of position on top of the buried grating. This variation is caused by interference with an optical field resulting from scattering by interface

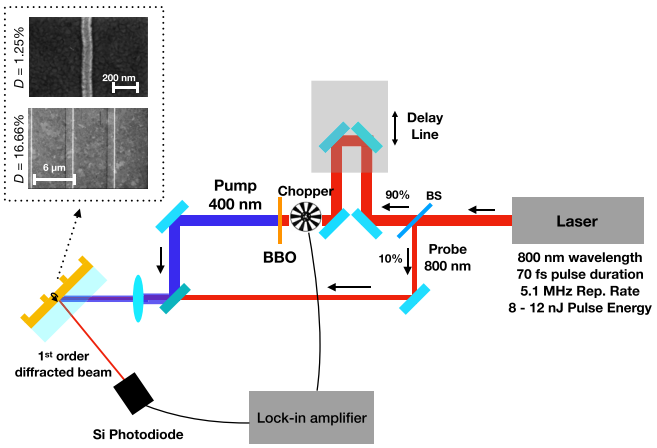

FIG. 1. Schematic of the experimental setup. The output from a 5.1 MHz repetition rate Ti:sapphire oscillator with a central wavelength of 800 nm is split into two parts. One beam (pump) is frequency doubled to a wavelength of 400 nm by a BBO crystal and modulated by a mechanical chopper at 6 kHz. The other beam (probe) has a central wavelength of 800 nm. The pump-induced first-order diffracted probe beam is measured by a silicon photodiode. The photodiode has a bandwidth of 50 kHz and its signal is sent to a lock-in amplifier, which uses as a reference the signal from the chopper. We show in the inset SEM images of the 16.66% and 1.25% duty cycle gratings, corresponding to 1 μm and 75 nm linewidths, respectively.

roughness.[20] The phase of this scattered field is random, resulting in a variation of the signal with the position. Therefore, for every sample, care was taken to choose a position on the sample where the signal is maximum. However, we point out that due to the statistical nature of the phase of the randomly scattered light, there is some uncertainty whether such a chosen maximum is an absolute maximum rather than a local maximum.[20] The signals shown in Fig. 2 are composed of a small sharp peak at zero delay for the 1 μm, 500 nm,and 250 nm linewidth gratings. We were not able to resolve this peak for the 125 nm and 75 nm linewidth samples because of the reduced signal-to-noise ratio. This peak is the result of a grating in the electron temperature near the interface, which leads to diffraction of the probe beam.[21] A few tens of picoseconds later, an oscillatory signal with a period of 50 ± 2 ps becomes apparent, lasting several hundreds of picoseconds. The amplitude of the oscillation decreases with the duty cycle of the gratings but, remarkably, a signal is still observed for the 1.25% duty cycle grating where the lines are only 75 nm wide. The diffracted signals all periodically drop below the signal level measured for negative time delays. This is the result of interference with a background optical field, caused by scattering of the probe electric field by surface roughness.[20] In order to check if the thickness of the Au layer influences the measurements, we also measured on a similar set of gratings fabricated on a thicker Au layer of 142 nm. In Fig. 3, we plot the diffracted signal measured as a function of the pump-probe delay for the five different gratings with linewidths of 1 μm, 500 nm, 250 nm, 125 nm, and 75 nm (solid colored lines in top five panels). In contrast to the measurements performed on the gratings on the 90 nm thick Au layer, here we observe a longer oscillation period of about 89 ± 3 ps and a somewhat faster signal decay. Around zero delay, a diffraction peak caused by an electron temperature grating is barely visible in the measurements. We note that a weaker diffraction signal due to

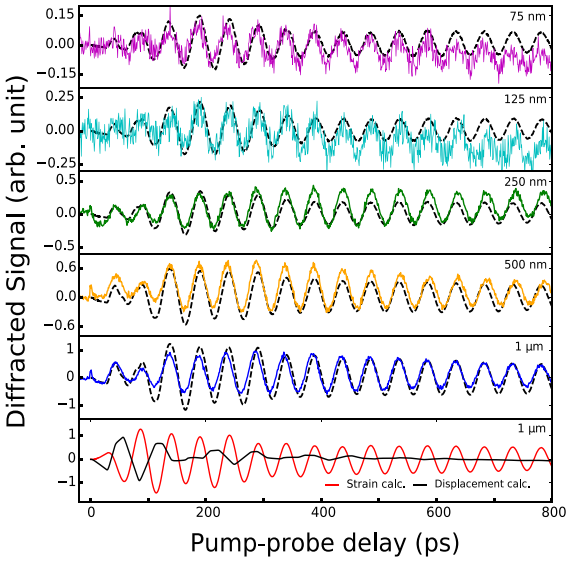

FIG. 2. The measured first-order diffracted probe signal as a function of pump-probe time delay for the five Au gratings fabricated on a 90 nm thick Au layer. The linewidths of the gratings vary from 75 nm to 1 μm. The period of all gratings is 6 μm and the amplitude is 44 nm. The dashed curves are the numerically calculated diffraction signals as a function of pump-probe delay. In the bottom panel, numerical calculations of the diffracted signals as a function of pump-probe time delay are shown, taking *only* surface displacement at the glass/Au interface into account (black line) or *only* diffraction off the acoustic waves in glass (red line).

heating of the electron gas is expected here, since the electron gas temperature grating is weaker for a thicker Au layer.[21] We can observe in the measurements that the diffracted signal strength decreases with the duty cycle. To quantify this trend, we plot in Fig. 4 the peak-to-peak amplitude of the signal from the first

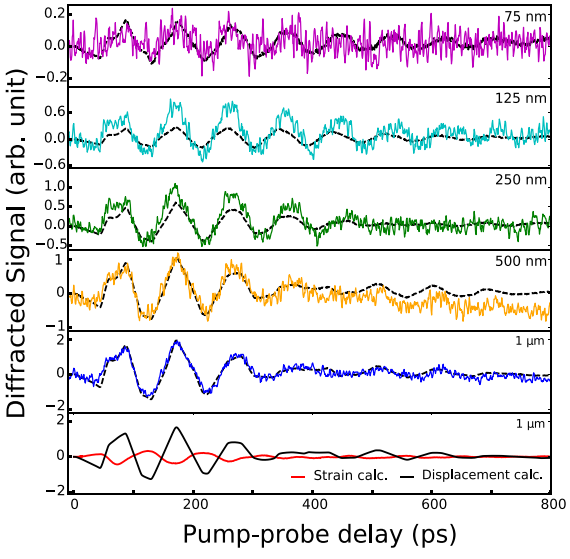

FIG. 3. The same as Fig. 2 but for the five different gratings fabricated on the 142 nm thick Au layer.

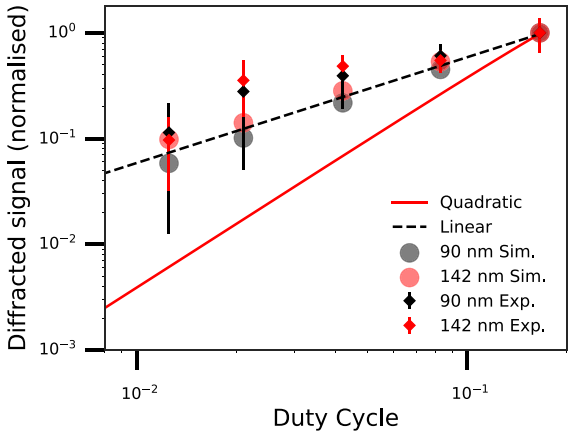

FIG. 4. Normalized diffracted signal, taken here as the amplitude of the first positive diffraction peak, as a function of duty cycle, measured (black and red diamonds) and numerically calculated (gray and red dots) for the five gratings on a 90 nm and a 142 nm thick Au layer, respectively.

acoustic reflection as a function of the duty cycle of the five gratings deposited on 90 nm Au layer and on 142 nm Au layer. The data have been normalized by dividing all diffracted signals by the value for the 16.66% duty cycle (1 μm linewidth) sample. As Chang *et al.* showed, for nonzero diffraction orders, the diffraction efficiency of a binary grating should be proportional to the square of the duty cycle, for low values of the duty cycle.[22] Surprisingly, in our experiment, we find that the signal does not scale quadratically with the duty cycle. We observe a dependence that is closer to a linear dependence, indicated by the dashed line.

In order to confirm that our interpretation of the measurements is correct, we also performed extensive calculations of the diffracted signal. For this, we use the numerical model of Zhang *et al.*[23] This is a 2D numerical model, which contains all the steps involved in a typical photoacoustic experiment, such as generation, propagation, and detection of the acoustic waves. In Figs. 2 and 3 (black dashed curves), we plot the diffracted signals, calculated for the gratings on 90 nm and 142 nm thick Au layers. Calculations were first carried out for the samples with the 1 μm linewidth as these provided the strongest signals. Parameters were manually adjusted until the best fit between the measurements and the calculations was obtained for the first diffraction peak. Then, without changing parameter values, calculations were performed for the lower duty cycle gratings as well. All curves were normalized by dividing them by the maximum value calculated for the 16.66% duty cycle grating (1 μm linewidth). The calculations show oscillatory long-lasting signals with a period of about 50 ps for all gratings on the 90 nm thick Au layer and of about 89 ps for the gratings on the 142 nm thick Au layer. The amplitudes of the signals decrease with the duty cycle of the gratings, and all calculations are in reasonable to good agreement with the experimental results. In the bottom panels of Figs. 2 and 3, we plot the calculated diffracted signal from *only* the Au surface displacement at the glass/Au interface (black curve) and from *only* the acoustic grating propagating inside the glass (strain, red curve) for the 1 μm linewidth sample. The oscillatory nature of the latter is sometimes also referred to as time-domain Brillouin scattering.[24] Here too, the same constant background field as

used in the full calculations is assumed to be present. The calculated curves clearly show that, particularly at long time delays, the signal is dominated by the strain contribution for the gratings on the 90 nm thick Au layer. As for the gratings on the 142 nm thick Au layer, we find that the displacement of the atoms at the glass/Au interface provides the strongest contribution to the measured signals.

A striking difference between the time-dependent diffraction for the gratings on the 90 nm layer and the 142 nm thick Au layers is that for the latter, the ~50 ps period oscillatory signal caused by Brillouin scattering is more or less absent in the measurements. This strongly suggests that for the 142 nm thick layer, the contribution to the diffracted signal of the acoustic wave propagating in glass is smaller than the contribution from the acoustic wave-induced atomic displacement at the glass/Au interface. This is supported by the numerical calculations of the diffracted signals. The strength of the optical diffraction signal caused by interface displacement depends on the amplitude of the displacement itself. Even though a glass/gold interface is different from an air/gold interface, the displacement responses are very similar. The reason for this is that the glass is essentially a "soft" material so that the interface is relatively free to move under the influence of a strain wave, similar to the air/gold interface. In contrast to the air/gold interface, however, the glass/gold interface partially transmits sound waves into the glass. This is nearly impossible at the air/gold interface where the acoustic impedance mismatch between gold and air at GHz frequencies is enormous. All these effects and physical properties are included in the numerical model that we use to simulate the measurements.

In our measurements, we find that the diffraction signal does not scale quadratically with the duty cycle of the gratings. From Chang *et al.*,[22] for a binary grating with a low value of the duty cycle D, the diffraction efficiency of the first-order diffracted beam, defined as the ratio between the power of the first-order diffracted light beam and that of the incident beam, can be approximated by

$$\eta \approx 2A^2(1-\cos\psi)D^2, \tag{1}$$

where A corresponds to the reflectance of the metal of the grating (A = 0 for no reflection and A = 1 for perfect reflection). ψ represents the phase difference between light reflected from the valleys and the peaks of the grating.

Equation (1) clearly shows that the diffraction efficiency should have a quadratic dependence on the duty cycle of the grating. In Fig. 4, this quadratic dependence is illustrated by the red line. However, the measured diffracted signal strength vs duty cycle is closer to a linear than a quadratic dependence. This can be understood by first realizing that the intensity of the field diffracted off the acoustic grating, E_{ac}^2, is proportional to the diffraction efficiency. From Eq. (1), we obtain $E_{ac}^2 \propto \eta \propto D^2$ and thus $E_{ac} \propto D$. Due to the presence of the background scattered field E_b, the ϕ-dependent oscillatory part of the total optical power is not proportional to E_{ac}^2, but to the cross term, $2E_bE_{ac}\cos(\phi) \propto D$, which dominates the measured signal because $E_b \gg E_{ac}$. In other words, due to the background scattered field E_b, the diffracted signal measured by the photodiode and filtered by the lock-in amplifier should scale *linearly* with the duty cycle, in agreement with our measurements. We note, however, that Eq. (1) is valid for binary (square wave) gratings only. According to diffraction theory, when the size of an object becomes comparable to or smaller than the wavelength of the wave, diffraction becomes significant.[25]

The acoustic wave that diffracts off the narrow lines has spread out by the time it reaches the interface such that the acoustic wave-induced grating can no longer be considered a binary grating. Thus, in our experiments, for grating lines on the order of or smaller than the acoustic wavelength, which is 180 nm for the 90 nm Au layer and 282 nm for the 142 nm Au layer, the acoustic grating replicas at the glass/metal interface should not be square-wave-like copies of the buried ones anymore for the thinnest grating lines. As a result, for the lowest duty cycle samples, it is not directly obvious that this linear trend should still hold. However, full numerical calculations that take acoustic diffraction into account also show that the diffracted signal vs duty cycle remains close to a linear dependence, as shown by the gray and red dots in Fig. 4. The calculated interface displacement profiles (not shown here) deviate somewhat from the ideal binary shape due acoustic diffraction, especially for the lowest duty cycle gratings. However, these changes have little effect on the diffracted signal strength. It is interesting to get an estimate of the amplitudes of the glass/Au interface displacement gratings and of the corresponding first-order diffraction efficiencies of these gratings, assuming no background field would be present and ignoring deviations from the shape of a perfect binary grating. From the numerical calculations, we find that the estimated peak-to-valley amplitude of the gratings fabricated on the 90 nm thick Au layer ranges from 14.1 pm for the 75 nm linewidth sample to 52.6 pm for the 1 μm linewidth sample. Using Eq. (1), this gives us estimated diffraction efficiencies η from $\sim 1.72 \times 10^{-11}$ to $\sim 4.07 \times 10^{-8}$, respectively. For the 142 nm thick Au sample, the amplitude of the interface displacement gratings is slightly smaller, ranging from 8.6 to 33.5 pm for the 75 nm and 1 μm linewidth samples, respectively. Again using Eq. (1), we estimate that this corresponds to diffraction efficiencies of $\sim 6.4 \times 10^{-12}$ and $\sim 1.7 \times 10^{-8}$. These calculated diffraction efficiencies are quite small and would be challenging to measure, especially for the 75 nm linewidth samples. Fortunately, we are still able to detect the buried gratings due to the presence of the scattered background optical field, which coherently amplifies the optical signal diffracted by the acoustic wave.

We have shown that ultrahigh-frequency sound waves, generated with femtosecond laser pulses, can be used to detect gratings buried underneath optically opaque layers. In our experiments, these sound waves are reflected off the buried grating and acquire a spatially periodic acoustic phase. When these acoustic waves reach the glass/metal interface, they displace the atoms at the interface, thereby forming a grating that can be detected by diffraction of a delayed probe pulse. By varying the duty cycle of the gratings, we have shown that gratings with linewidths as narrow as 75 nm can be detected. We find that the diffracted signals are composed of contributions from the grating-shaped acoustic waves in the metal, diffraction caused by Brillouin scattering, and a background field caused by scattering from interface roughness. This background optical field interferes with the optical fields diffracted by the acoustic waves in the metal and the glass and thus can weaken or enhance the diffracted signals. As a result, the predicted maximum diffracted signal strength as a function of duty cycle changes from a quadratic dependence to a linear dependence.

For wafer alignment applications, the unpredictability of the phase of the scattered light, which can vary from position to position and from layer to layer, can be a disadvantage. However, the relative influence of scattered light could be decreased by increasing the strength of the acoustic wave-induced diffraction by enhancing the

contrast between the acoustic waves reflected off the valleys and the ridges of the grating by fabricating larger-amplitude buried gratings. The influence of scattered probe light can also be diminished by using higher energy pump laser pulses, as probe diffraction scales quadratically with acoustic grating amplitude and, thus, pump-pulse energy, whereas the amount of probe light scattered by surface roughness would remain the same.

Our results illustrate the potential of photoacoustics to detect gratings with narrow lines buried below optically opaque layers.

DATA AVAILABILITY

The data that support the findings of this study are available from the corresponding author upon reasonable request.

REFERENCES

[1]A. Nolvi, I. Kassamakov, and E. Hæggström, "Subsurface metrology using scanning white light interferometry: Absolute z coordinates deep inside displays," J. Opt. Soc. Am. A **35**, A18–A22 (2018).

[2]M. H. van Es, A. Mohtashami, D. Piras, and H. Sadeghian, "Image-based overlay and alignment metrology through optically opaque media with sub-surface probe microscopy," Proc. SPIE **10585**, 105850R (2018).

[3]A. J. den Boef, "Optical wafer metrology sensors for process-robust CD and overlay control in semiconductor device manufacturing," Surf. Topogr. **4**, 023001 (2016).

[4]O. Matsuda, M. C. Larciprete, R. Li Voti, and O. B. Wright, "Fundamentals of picosecond laser ultrasonics," Ultrasonics **56**, 3–20 (2015).

[5]C. Thomsen, H. T. Grahn, H. J. Maris, and J. Tauc, "Surface generation and detection of phonons by picosecond light pulses," Phys. Rev. B **34**, 4129–4138 (1986).

[6]O. B. Wright and K. Kawashima, "Coherent phonon detection from ultrafast surface vibrations," Phys. Rev. Lett. **69**, 1668–1671 (1992).

[7]O. B. Wright and V. E. Gusev, "Acoustic generation in crystalline silicon with femtosecond optical pulses," Appl. Phys. Lett. **66**, 1190–1192 (1995).

[8]K. A. Nelson, R. J. D. Miller, D. R. Lutz, and M. D. Fayer, "Optical generation of tunable ultrasonic waves," J. Appl. Phys. **53**, 1144–1149 (1982).

[9]T. F. Crimmins, A. A. Maznev, and K. A. Nelson, "Transient grating measurements of picosecond acoustic pulses in metal films," Appl. Phys. Lett. **74**, 1344–1346 (1999).

[10]R. M. Slayton and K. A. Nelson, "Picosecond acoustic transmission measurements. Part I. transient grating generation and detection of acoustic responses in thin metal films," J. Chem. Phys. **120**, 3908–3918 (2004).

[11]C. Klieber, E. Peronne, K. Katayama, J. Choi, M. Yamaguchi, T. Pezeril, and K. A. Nelson, "Narrow-band acoustic attenuation measurements in vitreous silica at frequencies between 20 and 400 GHz," Appl. Phys. Lett. **98**, 211908 (2011).

[12]H. Maris, "Picosecond ultrasonics," Sci. Am. **278**, 86–89 (1998).

[13]T. Saito, O. Matsuda, and O. B. Wright, "Picosecond acoustic phonon pulse generation in nickel and chromium," Phys. Rev. B **67**, 205421 (2003).

[14]A. Huynh, N. D. Lanzillotti-Kimura, B. Jusserand, B. Perrin, A. Fainstein, M. F. Pascual-Winter, E. Peronne, and A. Lemaître, "Subterahertz phonon dynamics in acoustic nanocavities," Phys. Rev. Lett. **97**, 115502 (2006).

[15]T. Saito, O. Matsuda, M. Tomoda, and O. B. Wright, "Imaging gigahertz surface acoustic waves through the photoelastic effect," J. Opt. Soc. Am. B **27**, 2632–2638 (2010).

[16]C. J. K. Richardson, M. J. Ehrlich, and J. W. Wagner, "Interferometric detection of ultrafast thermoelastic transients in thin films: Theory with supporting experiment," J. Opt. Soc. Am. B **16**, 1007–1015 (1999).

[17]P. Ruello and V. E. Gusev, "Physical mechanisms of coherent acoustic phonons generation by ultrafast laser action," Ultrasonics **56**, 21– 35 (2015).

[18]M. Lejman, V. Shalagatskyi, O. Kovalenko, T. Pezeril, V. V. Temnov, and P. Ruello, "Ultrafast optical detection of coherent acoustic phonons emission driven by superdiffusive hot electrons," J. Opt. Soc. Am. B **31**, 282–290 (2014).

[19]S. Edward, H. Zhang, I. Setija, V. Verrina, A. Antoncecchi, S. Witte, and P. Planken, "Detection of hidden gratings through multilayer nanostructures using light and sound," Phys. Rev. Appl. **14**, 014015 (2020).

[20]V. Verrina, S. Edward, H. Zhang, A. Antoncecchi, S. Witte, and P. Planken, "Role of scattering by surface roughness in the photoacoustic detection of hidden micro-structures," Appl. Opt. (submitted).

[21]S. Edward, A. Antoncecchi, H. Zhang, H. Sielcken, S. Witte, and P. C. M. Planken, "Detection of periodic structures through opaque metal layers by optical measurements of ultrafast electron dynamics," Opt. Express **26**, 23380–23396 (2018).

[22]Y.-C. Chang, P. Zhou, and J. H. Burge, "Analysis of phase sensitivity for binary computer-generated holograms," Appl. Opt. **45**, 4223–4234 (2006).

[23]H. Zhang, A. Antoncecchi, S. Edward, I. Setija, P. Planken, and S. Witte, "Unraveling phononic, optoacoustic, and mechanical properties of metals with light-driven hypersound," Phys. Rev. Appl. **13**, 014010 (2020).

[24]O. Matsuda, T. Pezeril, I. Chaban, K. Fujita, and V. Gusev, "Time-domain Brillouin scattering assisted by diffraction gratings," Phys. Rev. B **97**, 064301 (2018).

[25]J. W. Goodman, "Fresnel and fraunhofer diffraction," in *Introduction to Fourier Optics*, 3rd ed. (Roberts & Company Publishers, 2005).